Minimization of dental implant diameter and length according to bone quality determined by finite element analysis and optimized calculation

Type of article: Original Article

Abbreviated title: Minimization of dental implant according to bone quality

Key Words: implant, bone quality, finite element analysis, mandible, optimization

Number of pages in the text: 29

Number of tables: 3

Number of figures: 5

Quantity of reprints: 0

Abstract

Purpose: The purpose of this study was to investigate the influences of bone quality and implant size on the maximum equivalent elastic strain (MES) in peri-implant bone using finite element (FE) analysis, and to minimize implant size via optimized calculation based on MES.

Methods: Three-dimensional FE models consisting of a mandible and a titanium implant with a superstructure were constructed and applied a vertical load or an oblique load of 60N. We investigated the effects of four variables: the thickness of the cortical bone (C), Young's modulus of the trabecular bone (T), and the diameter (D) and length (L) of the implant. According to the variables determined using Latin hypercube sampling, 500 FE models were constructed and analyzed under each of the loads following the construction of response surfaces with the MES as a response value. D and L were minimized by optimized calculation with the MES limited to the physiological limit with reference to the mechanostat theory.

Results: The MES was significantly influenced by D more than L, and could be restricted to the physiological limit unless both C and T were small.

Larger MES than physiological limit was observed around the bottom of implants

Conclusions: From the viewpoint of the mechanostat theory, we calculated minimum size of implants according to the bone quality. However, the results should be verified with more detailed FE models made using CT data, animal studies and clinical prognoses.

Key words: implant, bone quality, finite element analysis, mandible, optimization

1. Introduction

Diagnosis of the quality of bone is essential for dental implants. Both the Leckholm & Zarb [1] and Misch [2] classification systems of bone quality for dental implants are widely used as indices for planning implant treatment, and are based on CT and panoramic X-ray images.

It is obviously better to select implants that are as large as possible because of their better biomechanical features. However, the size or quality of bone may not allow implants with sufficient size. Although bone augmentation can make it possible to use implants with sufficient size, it also has problems such as invasiveness, the treatment period, graft materials, prognosis, the requirement for surgery and cost.

To diagnose the sufficient size of implants and/or the necessity of bone augmentation, a standard for the smallest size of implants in relation to the bone quality from the viewpoint of biomechanical features would be quite helpful.

Therefore, we investigated the influences of the thickness of the cortical bone and Young's modulus of the trabecular bone as typical variables indicating bone quality and the size of the implant on the strain in bone

around implants using finite element analysis (FEA) and optimized calculation combined with response surface methodology, and attempted to clarify the selection criteria for the implant size from the viewpoint of biomechanics. Hereafter, thickness of the cortical bone and Young's modulus of the trabecular bone are collectively referred to as just "bone quality".

2. Materials and methods

2.1 Finite Element Model

We created three-dimensional finite element models (Fig. 1) consisting of part of the mandible corresponding to the first molar and a titanium implant with the superstructure. The sizes of the mandible and the implant, including its thread height and size, were based on the literature, [3, 4] and the Brånemark MKIII RP (Brånemark System), respectively. The thread height and width of the implant were 0.3 mm and 0.6 mm, respectively (Fig. 2). The superstructure of the implant prosthesis was simplified and consisted of gold alloy. All components, the bone, the superstructure, the abutment, and the implant body, were assumed to be fixed to each other.

The models consisted of approximately 84,000 nodes and 80,000 hexahedron elements on average. All elements were homogenous and isotropic. The properties of the materials (Table 1) were based on previous studies. The nodes on the mesial and distal sections of the mandible were restrained in all directions.

2.2 Loading Conditions

The loading conditions simulated masticatory force. The loading point corresponded to the central fossa of the occlusal surface, and the total amount of the load was 60N. The load directions were twofold: a vertical load along the axis of the implant, and a oblique load directed 15 degrees lingually lower toward the implant axis (Fig. 1). Since the FE analysis was performed with the mesial (distal) half of the whole area considering the symmetry, the exact load in the analysis was reduced by half, i.e., 30N.

2.3 Variables

We investigated the influences of four variables: the thickness of the cortical bone (C), Young's modulus of the trabecular bone (T) and the diameter (D) and length (L) of the implant (Table 2). C was 0.5, 0.8, 1.1, 1.4, 1.7 or 2.0 mm. T ranged from 0.1 GPa to 1.5 GPa. D ranged from 3.5 mm to 6.0 mm. L was 8, 10, 11 or 13 mm.

2.4 Evaluation of FEA and response surface

FEA was performed using finite element software (MSC.Marc2010, MSC Software). We first investigated the relationships among the location of the

maximum equivalent strain in the peri-implant bone (MES), C and T with an implant 10mm long and 4.0mm in diameter. Next, the variables of the finite element model were assigned using Latin hypercube sampling to effectively avoid sample repetition. Five hundred models were constructed and analyzed under each load condition, following the construction of the response surface with the MES as the objective value. All of the procedures were done automatically using optimization software (Optimus 10.3, Cybernet Systems). The relationship between the maximum strain and each variable was investigated considering the response surface, a kind of higher degree regression equation. In the construction of the response surface, each FE analysis was given variables by means of Latin hypercube sampling so that the dispersion of the variables showed a normal distribution to minimize the statistical error. The response surface could be displayed as a curved surface if two arbitrary variables were selected from C, T, D and L.

2.5 Optimized calculation

Based on the response surface, the diameter and length of the implant were minimized while keeping the maximum strain within 3000 microstrains,

which is the physiological limit in the mechanostat theory [5, 6] , by optimized calculation. The length and diameter of the implant were minimized independently to 10 mm and 4.0 mm, respectively, with the other variables kept constant.

3. Results

3.1 FEA

Examples of the results of FEA are shown in Fig. 3. The relationships between the bone quality and the location of the MES are shown in Fig. 4. The MES under the oblique load was greater than that under the vertical load. Under the oblique load, the equivalent strain was the largest in the trabecular bone around the bottom of the implant when T was less than about 0.45 GPa with the implant 10mm in length and 4.0mm in diameter. When T was more than about 0.75GPa, the equivalent strain was the largest in the trabecular bone around the neck of the implant. When T was between these values, this location of the MES depended on C (Fig. 4a). However, when the maximum implant size (13mm in length and 6.0mm in diameter) was selected, the boundary value was approximately 0.45GPa regardless of C (Fig. 4b).

3.2 Response surface

Figs. 5a and 5b show the influences of C and T on the MES with response surfaces. The thinner C and the lower T were, the larger the equivalent

elastic strain was. The response surfaces presented in Figs. 5c and 5d show the influences of D and L. Since the slope of the response surface shows the rate of variability, D strongly influenced the MES in comparison to L.

3.3 Optimized calculation

Table 3 shows the results of the optimized calculation. The MES was maintained at less than 3000 microstrains by choosing a greater length or diameter for the implant, though the largest implant exceeded 3000 microstrains when both C and T were small. When T was more than approximately 0.5 GPa, which corresponds to 589HU, the MES was limited to 3000 microstrains with smaller implants. Practically, it was 8mm in length or 3.5mm in diameter under the vertical load. When T was more than approximately 0.6 GPa, which corresponds to 626HU, the MES was limited to 3000 microstrains with the 3.5 mm diameter implant under the oblique load. Since the MES under the oblique load was greater than that under the vertical load, it was difficult to limit the MES to within 3000 microstrains with an implant having maximum D and L under the oblique load when T was under 0.5 GPa.

4. Discussion

4.1 Material properties of bone

In Misch's classification, [2] class D3 bone is composed of a thick, porous layer of cortical bone in the alveolar crest and fine trabecular bone under the cortical bone. This type of bone can be found in the anterior maxilla and the posterior mandible. Its strength is 50% of that of D2 bone, which appears to be just right, not too hard or too soft, and suitable for implants. Class D4 bone is too weak for dental implants without surgical pretreatment. However, there may be comparatively many options for implant size in the case of D3 bone. Therefore, we assumed that the bone was class D3 in this study and determined that the Young's modulus of the trabecular bone ranged from 0.1 GPa to 1.5 GPa, which corresponds to from 344 to 850HU, [7, 8] for the D3 bone.

In this study, trabecular bone was assumed to be homogenous and isotropic, which differs from patient-specific FE models [9, 10] using real structures of trabecular bone from computed tomography data, and the anisotropic properties [11] of real bone. It would be clinically useful if patient-specific FE models could routinely be constructed easily for clinical diagnosis of bone

quality with a lower cost. However, some problems still remain. [9, 10] Thus, simplified models applicable to every case are considered to be better to investigate the general influence of bone properties. Because of this simplification, the results of this study should be verified with patient-specific models in the future.

On the other hand, there are some variations of the material properties of cortical bone. [12] However, we fixed the material properties for cortical bone because we could not find obvious effects of the material properties of the bone on the strain in the bone around implants in our preliminary analysis.

4.2 Amount of bone and height of the superstructure

In this study, we determined the height of the superstructure according to the average height of the crown of the first molars with no reduction of alveolar bone. However, the height of the superstructure depends on the horizontal level of alveolar bone. Highly absorbed bone results in high superstructures and aggravates the crown-to-implant ratio, which may cause concentration of stress and strain in bone. This point should be taken into account as a limitation of this study.

4.3 Loading conditions

In most FE studies [13-16], stress and strain in bone were evaluated under the maximum occlusal load or a larger load than that in our study. However, in the mechanostat theory, the assumed load is the “typical peak voluntary mechanical loads that refers to the largest repeated and intentional loads on bones exerted by intentional activities during a typical week or month”. [5] If we apply this theory to evaluate strain in bone, the amount of load should be determined according to the largest masticatory force and be smaller than with maximum clenching.

Gibbs et al. [17] measured occlusal force using the sound transmission method and reported that maximum occlusal forces during chewing were generated during maximum intercuspation and averaged 26.7 kgf (262N). Kumagai et al. [18] recorded the occlusal force distribution in the intercuspal position with the Dental Prescale System, a computerized analysis system for the evaluation of occlusal load using a color-developing chemical reaction, under management with electromyography. They reported that the occlusal force was 200N at 20% of maximum voluntary clenching. Hidaka et al. [19]

measured the occlusal force on each tooth during maximum voluntary clenching with the Dental Prescale System and reported the distribution of the occlusal force. Based on these references, loading of 60N was used as the masticatory force at the first molar.

Although there were some variations in the inclination in previous FEA studies, a few measured values were reported in the literature [16]. According to the lateral component of masticatory movement, it was considered to be impossible to avoid lateral force during mastication, even if occlusal contacts in lateral mandibular movements were not allowed. Therefore, on the assumption of an implant prostheses for a defect of the first molar, and no occlusal contacts in lateral movement, we selected a oblique load with a small angulation of 15 degrees.

4.4 Mechanostat theory

We evaluated the equivalent bone strain as the absolute value based on the mechanostat theory of Frost [5, 6]. Based on experimental results, he advocated mechanical strain as the parameter determining bone remodeling.

He reported that 3000 microstrains approximately equals bone's yield point. It was the threshold strain range that caused microscopic fatigue damage in bone, in and above which unrepaired damage could begin to accumulate. This theory has been verified in an animal study with finite element analysis and reported to be efficient. [20, 21] It is the only criterion that is commonly used for absolute biomechanical evaluation of bone. [22-24] In their systematic review on the strain measurements in human bone, Al Nazer et al. [25] reported that most of the strains measured in vivo in different bones were generally within the physiological loading zone defined by the mechanostat theory. We therefore consider 3000 microstrains to be the physiological limit based on this theory.

4.5 FEA

From the results of FEA, we found that the MES occurred in the peri-implant bone around the bottom or the neck of the implant according to the difference in T, which is consistent with previous studies. [23, 24, 26] However, most FE studies [13-16, 22, 26-31] show the stress concentration around the neck of the implant. In these FE studies, Young's modulus of

trabecular bone is approximately 0.5GPa or more with rare exceptions [24, 32], in which the strain/stress concentration around the bottom of the implants is shown, although patients, whose trabecular bone of the mandible is assumed to have a Young's modulus of less than 0.5GPa do exist. [24] However, if bone quality is relatively poor, clinicians should consider bone augmentation, or may give up on the implant prosthesis itself. The healthy animals used in the experiment were hardly considered to have bone of poor quality. Thus, the results of this study may be due to the relatively low density of trabecular bone. The boundary area of the bone quality where the location of the MES changed that we showed in this study needs verification with more detailed FE models and animal studies.

4.6 Response surface

Response surface methodology (RSM) is a method using mathematical and statistical techniques. Its objective is to understand influences of experimental variables on the response variable with minimal samples. The application of RSM to design optimization is aimed at reducing the cost of analysis. Venter et al. [33] have discussed the advantages of using RSM for design optimization problems and reported that RSM could provide a

perspective from minimal numbers of experiments.

From the response surface obtained, we found that bone strain decreased with increases of D and L. D played a more important role than L in reducing bone strain. Thus, more attention should be paid to implant diameter when the bone is of poor quality. Previous studies [34, 35] constructed response surfaces and showed the same tendency as our results. However, the maximum von Mises stresses, which they focused on, could only be evaluated qualitatively, not quantitatively, for biomechanical suitability. On the other hand, the maximum equivalent strain, which we focused on in this study, could be evaluated quantitatively from the viewpoint of the mechanostat theory. [5, 6] Therefore, we could suggest concrete sizes that might be clinically applicable for implants according to bone quality.

Comparing Figs. 4a and 5b, the relationship between the MES and its location became clear. When the MES was larger than 3000 microstrains, it always occurred in the bone around the bottom of the implant. Therefore, limiting the strain there might lead to improvement of the biomechanical condition of the bone around implants.

4.7 Optimized calculation

The methods of optimization have been used in manufacturing industries and have been applied in the field of the dental implants recently. [27-29, 35] Optimization is the determination of the best answer to satisfy a constraint condition. Previous studies [22, 30, 31] reported the effects of diameter and length on implant stability and their importance for success. We found that, with increases of D and L, bone strain decreased, which is consistent with their studies. The optimized calculations provided a minimum size for the implant satisfying the conditions, but the implant size should also take other conditions into account (e.g., anatomical limitations). D3 bone seemed to be suitable for implants; however, based on our results, some D3 bone might be unsuitable for implants in the mandible with extremely thin cortical bone. It may be necessary to consider the condition of occlusion and other factors. These results can be applied in the treatment planning and design for the implant.

4.8 Prospects for the future

The condition of the bone when the MES occurred around the bottom of the

implant essentially corresponded to that when the MES exceeded 3000 microstrains. In other words, excessive MES was considered to occur around the bottom of the implant. Under the conditions of this study, it was hard to control the equivalent elastic strain concentrated around the bottom of the implant by magnification of the implant. For more improvement, implant shapes that lead to restriction of the strain around the bottom of the implant should be investigated by means of shape optimization.

4.9 Limitations of the study

We investigated the relationships among bone quality, quantity, implant length and diameter from the perspective of biomechanics and found a certain tendency with regard to the MES. However, since the results of this study were obtained from simplified FE models, it was necessary to verify with patient-specific models using CT data, which vary with bone quality, and to compare our results with clinical prognoses. Although the present study proposes a minimized implant size with optimized calculation, it may be necessary to select a somewhat larger size clinically to ensure sufficient reliability and safety. It is necessary to verify the results of this study in

relation to the decisions of clinicians based on their experiences.

On the other hand, since the success of the implant depends on several factors such as bone quality, bone quantity, bone structure, implant design, implant displacement and more, [22, 36] it would to be better to include their influences. This is a problem that remains to be investigated in the future studies.

In this study, we assumed perfect osseointegration between the bone and the implant. However, previous studies [37, 38] reported that about 50 to 80% bone-implant contact is commonly observed with clinically successful implants. Kurniawan et al. [32] investigated the biomechanics of peri-implant bone that had different degrees of osseointegration with FEA and reported that a higher degree of osseointegration induced higher stress but lower strain. However, the ratio between the maximum strain and yield strain was not so significantly changed. Based on their results, it may therefore be safer clinically to select a slightly larger implant than indicated by our results.

5. Conclusion

We proposed a minimum size for implants according to the thickness of the cortical bone and Young's modulus of the trabecular bone, which can be obtained from computed tomography and converted. Implants of proper length or diameter could limit the maximum equivalent strain in peri-implant bone except when both the thickness of the cortical bone and the Young's modulus of the trabecular bone are small. When T was more than approximately 0.5 GPa, the MES was limited to 3000 microstrains with implants 8mm in length or 3.5mm in diameter under the vertical load. When T was more than approximately 0.6 GPa, the MES was limited with implants 3.5 mm in diameter under the oblique load. In other cases, the reduction of the strain in bone around the bottom of implants may be the key to extend the adaptability of implants to poor quality bone. However, these results should be verified with more detailed FE models made using CT data, animal studies and clinical prognoses.

Authorship

NU participated in the design of the study and the construction of FE models, and carried out the final calculation and the optimization. YT participated in the construction of the FE models and programming for the optimization. AY participated in the construction of FE models. All authors read and approved the final manuscript.

Acknowledgements

This study was supported by the grant-in-aid for Scientific Research of Japan Society of the Promotion of Science (No 24592892).

Conflict of interest statement

The authors declare no conflict of interest for this study.

References

[1] Lekholm U, Zarb GA, Albrektsson T. Patient selection and preparation. Tissue Integrated Prostheses: Osseointegration in Clinical Dentistry. Chicago: Quintessence, 1985:199-209.

[2] Misch CE. Bone dentistry: A Key Determinant for Clinical Success. Contemporary implant dentistry: Mosby, 1999:109-118.

[3] Geng JP, Tan KB, Liu GR. Application of finite element analysis in implant dentistry: a review of the literature. J Prosthet Dent 2001;85:585-598.

[4] Van Staden RC, Guan H, Loo YC. Application of the finite element method in dental implant research. Comput Methods Biomech Biomed Engin 2006;9:257-270.

[5] Frost HM. Bone's mechanostat: a 2003 update. Anat Rec A Discov Mol Cell Evol Biol 2003;275:1081-1101.

[6] Frost HM. A 2003 update of bone physiology and Wolff's Law for clinicians. Angle Orthod 2004;74:3-15.

[7] Les CM, Keyak JH, Stover SM, Taylor KT, Kaneps AJ. Estimation of Material Properties in the Equine Metacarpus with Use of Quantitative Computed-Tomography. J Orthopaed Res 1994;12:822-833.

[8] Keyak JH, Lee IY, Skinner HB. Correlations between Orthogonal Mechanical-Properties and Density of Trabecular Bone - Use of Different Densitometric Measures. J Biomed Mater Res 1994;28:1329-1336.

[9] Pankaj P. Patient-specific modelling of bone and bone-implant systems: the challenges. Int J Numer Method Biomed Eng 2013;29:233-249.

[10] Poelert S, Valstar E, Weinans H, Zadpoor AA. Patient-specific finite element modeling of bones. Proc Inst Mech Eng H 2013;227:464-478.

[11]O'Mahony AM, Williams JL, Katz JO, Spencer P. Anisotropic elastic properties of cancellous bone from a human edentulous mandible. Clin Oral Implants Res 2000;11:415-421.

[12] Dechow PC, Nail GA, Schwartz-Dabney CL, Ashman RB. Elastic properties of human supraorbital and mandibular bone. Am J Phys Anthropol 1993;90:291-306.

[13] Qian L, Todo M, Matsushita Y, Koyano K. Effects of implant diameter, insertion depth, and loading angle on stress/strain fields in implant/jawbone systems: finite element analysis. Int J Oral Maxillofac

Implants 2009;24:877-886.
[14] Kong L, Gu Z, Li T, Wu J, Hu K, Liu Y, et al. Biomechanical optimization of implant diameter and length for immediate loading: a nonlinear finite element analysis. Int J Prosthodont 2009;22:607-615.
[15] Demenko V, Linetskiy I, Nesvit K, Shevchenko A. Ultimate masticatory force as a criterion in implant selection. J Dent Res 2011;90:1211-1215.
[16] Shigemitsu R, Ogawa T, Matsumoto T, Yoda N, Gunji Y, Yamakawa Y, et al. Stress distribution in the peri-implant bone with splinted and non-splinted implants by in vivo loading data-based finite element analysis. Odontology 2013;101:222-226.
[17] Gibbs CH, Mahan PE, Lundeen HC, Brehnan K, Walsh EK, Holbrook WB. Occlusal Forces during Chewing and Swallowing as Measured by Sound-Transmission. J Prosthet Dent 1981;46:443-449.
[18] Kumagai H, Suzuki T, Hamada T, Sondang P, Fujitani M, Nikawa H. Occlusal force distribution on the dental arch during various levels of clenching. J Oral Rehabil 1999;26:932-935.
[19] Hidaka O, Iwasaki M, Saito M, Morimoto T. Influence of clenching intensity on bite force balance, occlusal contact area, and average bite pressure. J Dent Res 1999;78:1336-1344.
[20] Levchuk A, Zwahlen A, Weigt C, Lambers FM, Badilatti SD, Schulte FA, et al. The Clinical Biomechanics Award 2012 - presented by the European Society of Biomechanics: large scale simulations of trabecular bone adaptation to loading and treatment. Clin Biomech 2014; 29:355-362.
[21] Mahnama A, Tafazzoli-Shadpour M, Geramipanah F, Mehdi Dehghan M. Verification of the mechanostat theory in mandible remodeling after tooth extraction: animal study and numerical modeling. J Mech Behav Biomed Mater 2013;20:354-362.
[22] Chou HY, Muftu S, Bozkaya D. Combined effects of implant insertion depth and alveolar bone quality on periimplant bone strain induced by a wide-diameter, short implant and a narrow-diameter, long implant. J Prosthet Dent 2010;104:293-300.
[23] Kan JP, Judge RB, Palamara JE. In vitro bone strain analysis of implant following occlusal overload. Clin Oral Implants Res 2014;25:e73-82.
[24] Sugiura T, Yamamoto K, Kawakami M, Horita S, Murakami K, Kirita T. Influence of bone parameters on peri-implant bone strain distribution in

the posterior mandible. Med Oral Patol Oral Cir Bucal 2015:e66-e73.
[25] Al Nazer R, Lanovaz J, Kawalilak C, Johnston JD, Kontulainen S. Direct in vivo strain measurements in human bone-a systematic literature review. J Biomech 2012;45:27-40.
[26] Tada S, Stegaroiu R, Kitamura E, Miyakawa O, Kusakari H. Influence of implant design and bone quality on stress/strain distribution in bone around implants. Int J Oral Maxillofac Implants 2003;18:357-368.
[27] Li T, Hu K, Cheng L, Ding Y, Ding Y, Shao J, et al. Optimum selection of the dental implant diameter and length in the posterior mandible with poor bone quality – A 3D finite element analysis. Appl Math Model 2011;35:446-456.
[28] Li T, Kong L, Wang Y, Hu K, Song L, Liu B, et al. Selection of optimal dental implant diameter and length in type IV bone: a three-dimensional finite element analysis. Int J Oral Maxillofac Surg 2009;38:1077-1083.
[29] Ao J, Li T, Liu Y, Ding Y, Wu G, Hu K, et al. Optimal design of thread height and width on an immediately loaded cylinder implant: a finite element analysis. Comput Biol Med 2010;40:681-686.
[30] Baggi L, Cappelloni I, Di Girolamo M, Maceri F, Vairo G. The influence of implant diameter and length on stress distribution of osseointegrated implants related to crestal bone geometry: a three-dimensional finite element analysis. J Prosthet Dent 2008;100:422-431.
[31] Okumura N, Stegaroiu R, Kitamura E, Kurokawa K, Nomura S. Influence of maxillary cortical bone thickness, implant design and implant diameter on stress around implants: a three-dimensional finite element analysis. J Prosthodont Res 2010;54:133-142.
[32] Kurniawan D, Nor FM, Lee HY, Lim JY. Finite element analysis of bone-implant biomechanics: refinement through featuring various osseointegration conditions. Int J Oral Maxillofac Surg 2012; 41:1090-1096.
[33] Venter G, Haftka RT. Using response surface approximations in fuzzy set based design optimization. Struct Optimization 1999;18:218-227.
[34] Kong L, Sun Y, Hu K, Li D, Hou R, Yang J, et al. Bivariate evaluation of cylinder implant diameter and length: a three-dimensional finite element analysis. Journal of prosthodontics : official journal of the American College of Prosthodontists 2008;17:286-293.
[35] Gao Y, Li YF, Shao B, Li T, Xia N, Xu LX, et al. Biomechanical

optimisation of the length ratio of the two endosseous portions in distraction implants: a three-dimensional finite element analysis. The British journal of oral & maxillofacial surgery 2012;50:e86-92.

[36] Mohammed Ibrahim M, Thulasingam C, Nasser KS, Balaji V, Rajakumar M, Rupkumar P. Evaluation of design parameters of dental implant shape, diameter and length on stress distribution: a finite element analysis. Journal of Indian Prosthodontic Society 2011;11:165-171.

[37] Degidi M, Petrone G, Lezzi G, Piattelli A. Histologic evaluation of 2 human immediately loaded and 1 titanium implants inserted in the posterior mandible and submerged retrieved after 6 months. The Journal of oral implantology 2003;29:223-229.

[38] Testori T, Szmukler-Moncler S, Francetti L, Del Fabbro M, Trisi P, Weinstein RL. Healing of Osseotite implants under submerged and immediate loading conditions in a single patient: a case report and interface analysis after 2 months. The International journal of periodontics & restorative dentistry 2002;22:345-353.

Legend to Figures

Fig. 1. Finite element model and loading points and directions

Axis-X: buccal, Y: coronal, Z: mesial (or distal)

Fig. 2. An example of the finite element model of an implant

(W) Thread width; (H) thread height

Fig. 3. The results of finite element analysis (equivalent elastic strain)

(a) vertical load; (b) oblique load

Figs. 4. The relationship between the bone quality and the location of MES under oblique load

Black circles: MES occurred around the bottom of the implant

White circles: MES occurred around the neck of the implant

(a) Implant 10mm in length and 4.0mm in diameter.

(b) Implant 13mm in length and 6.0mm in diameter

Fig. 5. Response surfaces

The height at the intersection of arbitrary values C and T indicates the MES according to those variables, and is indicated by the seven contour colors, which divide 12,000 microstrain evenly, for convenience of understanding.

(a) The relationships between C and T under vertical loads

(b) The relationships between C and T under oblique loads

(c) The relationships between D and L under vertical loads

(d) The relationships between D and L under oblique loads

Table 1. Material properties of the finite element model

Materials	Young's modulus（GPa)	Poisson's ratio
gold alloy	100	0.3
implant(Titanium)	110	0.3
cortical bone	13.7	0.3
trabecular bone	0.1～1.5	0.3

Table 2. Variables of the finite element model

Variables	Range
thickness of cortical bone（mm)	0.5～2.0（6 types）
Young's modulus of trabecular bone (GPa)	0.1～1.5 (continuous variables)
length of the implant(mm)	8～13（4 types）
diameter of the implant(mm)	3.5～6.0（continuous variable）

Table 3. The results of optimized calculations

(a)

	Young's modulus of the trabecular bone(GPa)					
thickness of the cortical bone(mm)	0.1	0.35	0.6	0.85	1.2	1.5
0.5	>13*	8	8	8	8	8
0.8	>13*	8	8	8	8	8
1.1	>13*	8	8	8	8	8
1.4	11	8	8	8	8	8
1.7	8	8	8	8	8	8
2	8	8	8	8	8	8

(b)

	Young's modulus of the trabecular bone(GPa)					
thickness of the cortical bone(mm)	0.1	0.35	0.6	0.85	1.2	1.5
0.5	>6.0*	3.8	3.5	3.5	3.5	3.5
0.8	>6.0*	3.5	3.5	3.5	3.5	3.5
1.1	5.4	3.5	3.5	3.5	3.5	3.5
1.4	4.9	3.5	3.5	3.5	3.5	3.5
1.7	3.7	3.5	3.5	3.5	3.5	3.5
2	3.5	3.5	3.5	3.5	3.5	3.5

(c)

	Young's modulus of the trabecular bone(GPa)					
thickness of the cortical bone(mm)	0.1	0.35	0.6	0.85	1.2	1.5
0.5	>13*	>13*	13	10	8	8
0.8	>13*	>13*	11	8	13	13
1.1	>13*	>13*	8	10	13	13
1.4	>13*	>13*	10	13	13	13
1.7	>13*	>13*	10	13	13	8
2	>13*	>13*	10	13	13	8

(d)

	Young's modulus of the trabecular bone(GPa)					
thickness of the cortical bone(mm)	0.1	0.35	0.6	0.85	1.2	1.5
0.5	>6.0*	>6.0*	5.3	3.8	3.6	3.6
0.8	>6.0*	>6.0*	4.3	3.5	3.5	3.5
1.1	>6.0*	5.9	3.5	3.5	3.5	3.5
1.4	>6.0*	5.8	3.5	3.5	3.5	3.5
1.7	>6.0*	5.6	3.5	3.5	3.5	3.5
2	>6.0*	5.4	3.5	3.5	3.6	3.5

(a) Optimization of L in vertical load

(b) Optimization of D in vertical load

(c) Optimization of L in oblique load

(d) Optimization of D in oblique load

*Over 3000 microstrains when using maximum size of the implant under these analytical conditions

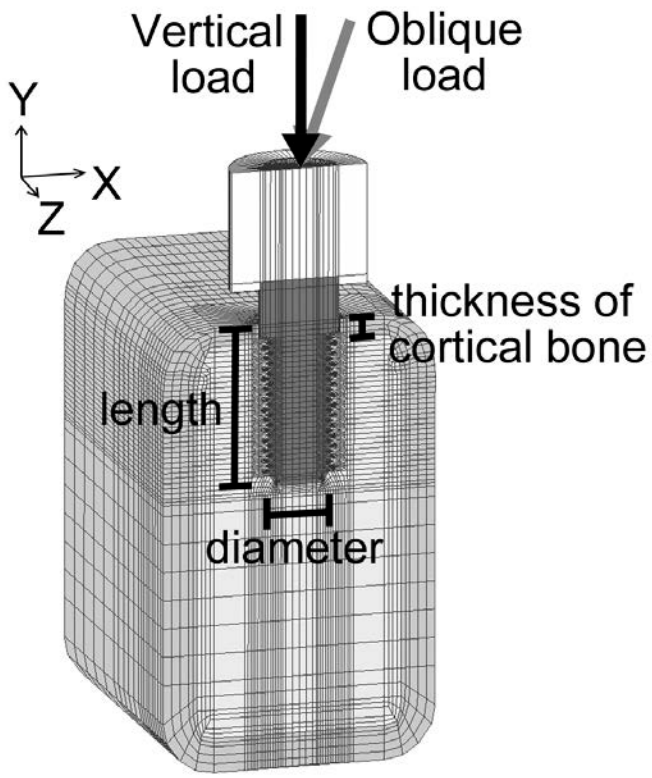
Vertical
load
Oblique
load
Y
X
Z
thickness of
cortical bone
length
diameter

Fig. 1

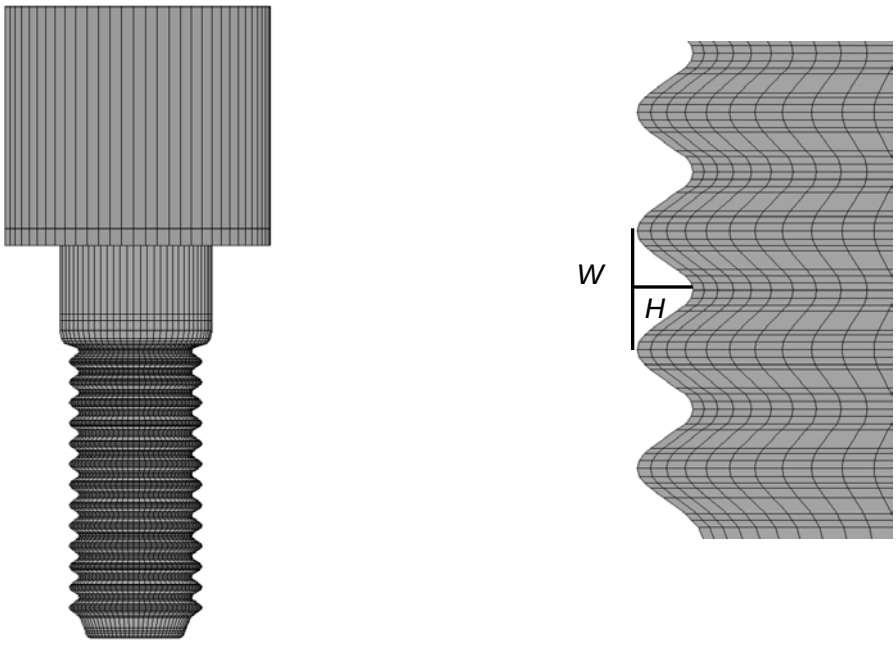

Fig. 2

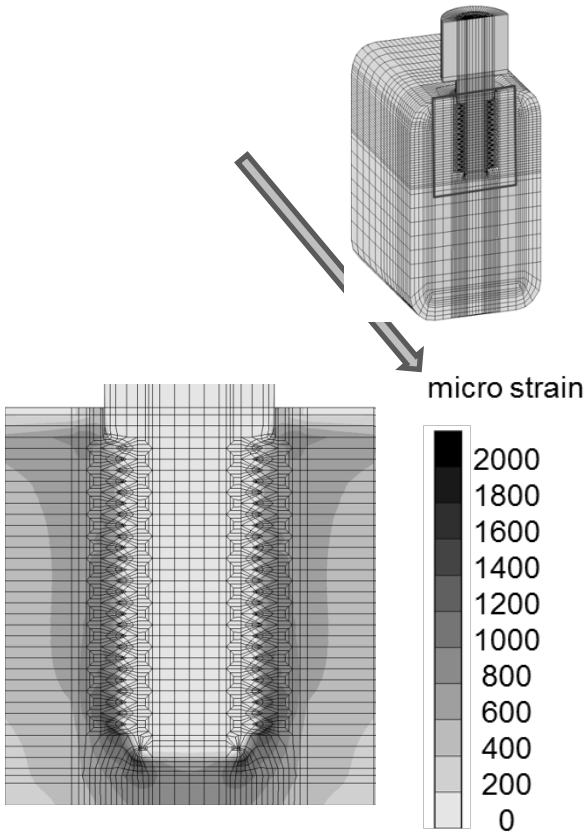

Fig. 3a

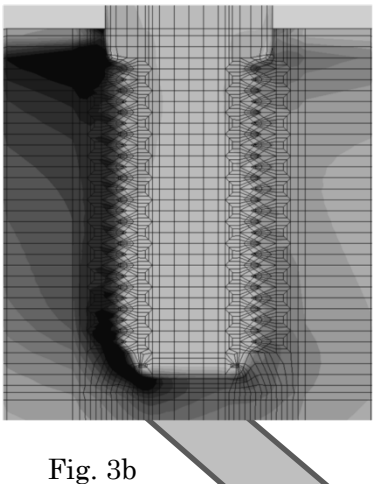

Fig. 3b

Fig. 3

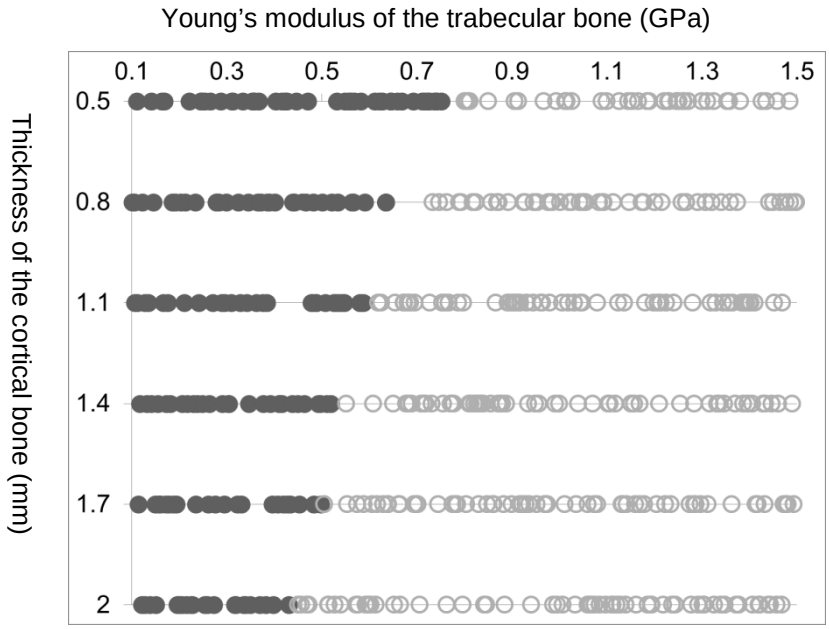

Fig. 4a

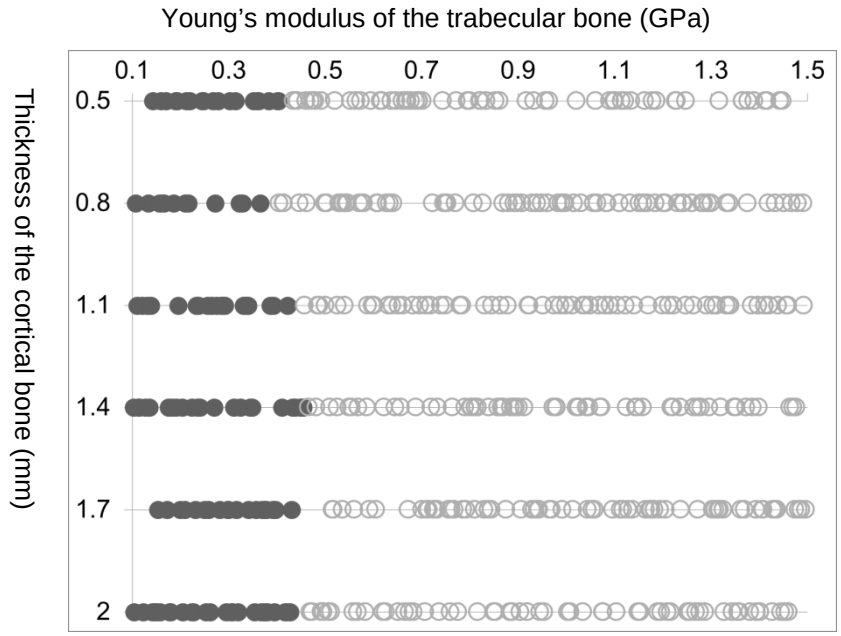

Fig. 4b

Figs .4

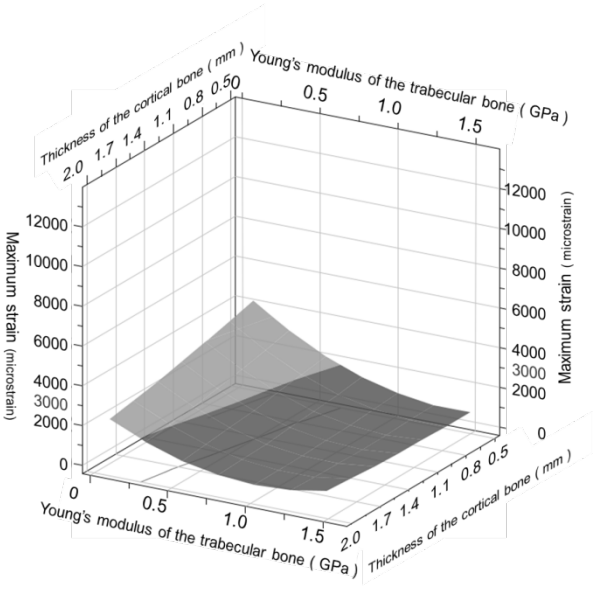

Fig. 5a

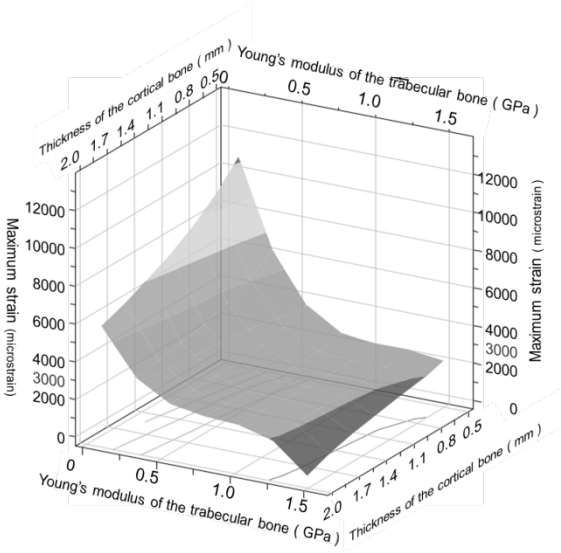

Fig. 5b

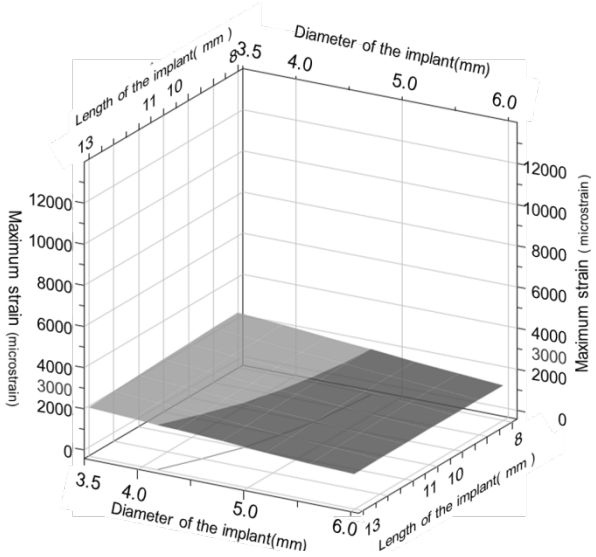

Fig. 5c

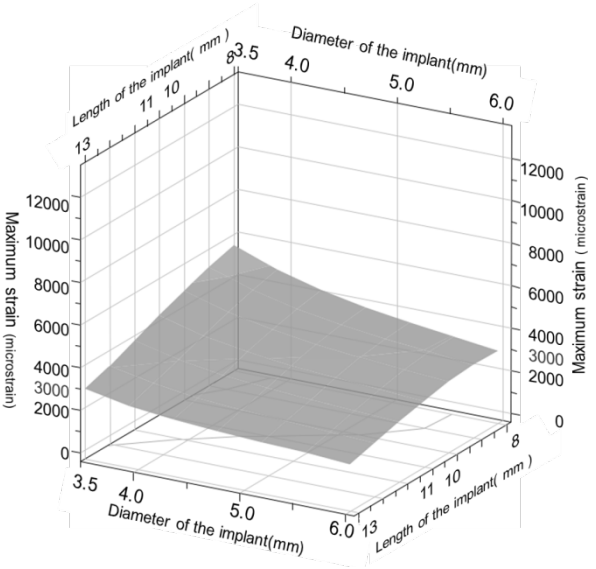

Fig. 5d

Fig. 5